The 2013 World Congress on
Advances in Structural Engineering and Mechanics (ASEM13)
Jeju, Korea, September 8-12, 2013

Fracture toughness of high performance concrete subjected to elevated temperatures: the effects of heating temperatures and testing conditions (hot and cold)

*Binsheng Zhang[1)], Martin Cullen[2)] and Tony Kilpatrick[3)]

[1), 2,), 3)] *School of Engineering and Built Environment*
Glasgow Caledonian University, Glasgow G4 0BA, United Kingdom
[1)] *Ben.Zhang@gcu.ac.uk*

ABSTRACT

In this study, the fracture toughness K_{IC} of HPC was determined by conducting three-point bending tests on eighty notched HPC beams of 500×100×100 mm at high temperatures up to 450ºC (hot) and in cooled-down states (cold). When the concrete beams exposed to high temperatures for 16 hours, both thermal and hygric equilibriums were achieved. K_{IC} for the hot concrete sustained a monotonic decrease tendency with the increasing heating temperature, with a sudden drop at 105ºC. For the cold concrete, K_{IC} sustained a two-stage decrease trend, dropping slowly with the heating temperature up to 150ºC and more rapidly thereafter. The fracture energy-based fracture toughness K_{IC}' was found to follow similar decrease trends with the heating temperature. The weight loss, the fracture energy and the modulus of rapture were also evaluated.

1. INTRODUCTION

In modern concrete constructions, e.g. tall reinforced concrete buildings, reinforced concrete cooling towers in thermal power plants, prestressed concrete pressure vessels in nuclear power stations, prestressed concrete silos in chemical factories, long prestressed concrete bridges, etc., high strength and ultra-high strength concrete has been largely used but the concrete needs to have ability to resist elevated temperatures. A higher concrete strength normally leads to a higher toughness but also increases the brittleness of concrete dramatically, which unavoidably causes concrete to fail very suddenly and even explosively. The information about fundamental properties such as strength, stiffness, toughness and brittleness under highly elevated temperatures is very often required. Besides strength and stiffness, the fracture toughness is a very useful fracture parameter for designing modern concrete structures, manufacturing high

[1), 2), 3)] Senior Lecturers

performance concrete materials, conducting structural analysis and simulations under various loading and environmental conditions, and assessing post-fire safety of reinforced and prestressed high strength concrete structures. Many investigations have been carried out to assess the fracture toughness of high performance concrete at room temperature, but the information about its performance at high temperatures is still limited. Extensive research into fracture properties of concrete at high temperatures only started about forty years ago and much progress has since been made [RILEM 1985; Schneider 1988; Bažant and Kaplan 1996; Phan and Carino 1998; Zhang et al 2000a, 2000b, 2000c; Cülfik and Özturan 2002; Peng et al 2006; Zhang and Bićanić 2006; Kanellopoulos et al 2009; Ulm and James 2011; Watanabe et al 2013].

High temperature influences the behaviour of concrete at different structural levels. At micro and meso concrete sustains physical and chemical changes. Physically, thermal dilations, thermal shrinkage and creep associated with water loss normally lead to large volume changes which can result in large internal stresses and strains such as interfacial thermal incompatibility and lead to micro cracking and fractures. Heating temperature also changes pore structures (porosity and pore size distribution) [Yan et al 2000]. High temperatures cause thermal and hygric gradients which lead to migration of water (diffusion, drying). Especially for high strength and high performance concrete with smaller porosity and pore sizes, rapid exposure to high temperatures can cause high pore pressure and lead to explosive spalling, which will be potentially disastrous [Bangi and Horiguchi 2011; Zhang et al 2013]. High temperatures also cause chemical and micro-structural changes, such as migration of water (diffusion, drying), increased dehydration, interfacial thermal incompatibility and chemical decomposition of hardened cement paste and aggregates. In general, exposure to high temperatures, the mechanical and structural characteristics of high performance concrete including strength, stiffness and toughness will be largely degraded.

Strength, stiffness, toughness and brittleness are all fundamental fracture properties for assessing the resistance of high performance concrete against cracking and fracture. Toughness commonly characterises the capacity of concrete to resist deformation and fracture so it is a synthetic property. By contrast, brittleness is commonly understood to the tendency for concrete to fracture rapidly before significant deformation occurs. Nowadays super high strength high performance with compressive strength over 250 MPa or even up to 300 MPa has been manufactured and applied into practical concrete construction [Nielson 1995; Haghighi et al 2007; Pu 2012]. To date, much research has been conducted on the strength and stiffness of high performance concrete at various heating scenarios [Felicetti and Gambarova 1998; Abe et al 1999; Zhang et al 2000a; Zhang and Bićanić 2002a, 2006; Chen and Liu 2004; Peng et al 2006; Watanabe et al 2013], and have found that the strength and stiffness of concrete decreased with increasing heating temperature, exposure time and thermal cycling. Some research has also been done on the toughness of high performance concrete [Zhang et al 2000b, 2000c; Nielson and Bićanić 2003; Zhang and Bićanić 2006; Kanellopoulos et al 2009; Watanabe et al 2013; Yu and Lu 2013]. As for the brittleness of high performance concrete at high temperatures, not much information is available. The characteristic length l_{ch} proposed by Hillerborg [Hillerborg et al. 1976] was used to assess the brittleness of normal- and high-strength concrete and was found to increase

with the increasing heating temperature and exposure time, which indicates that the concrete brittleness monotonically decreased with the increasing heating temperature and heating time [Zhang et al 2000a]. The ratio of the plastic and/or total energy/deformation to the elastic energy/deformation used as toughness indexes was also proposed to quantitatively assess the concrete brittleness and the same conclusions were drawn [Zhang et al 2000b, 2000c, 2002b].

Two parameters are generally used to assess the toughness of concrete, i.e. the fracture energy G_F and the fracture toughness K_{IC}, and they both increased with the increasing strength of concrete at room temperature. At high temperatures, G_F first increased with heating temperature until a transition point was reached and then gradually decreased [Bažant and Prat 1988; Baker 1996; Zhang et al 2000a]. The temperature corresponding to this point was found to be 300ºC for siliceous gravel concrete [Zhang and Bićanić 2002a] and basalt dolerite concrete [Zhang and Bićanić 2006]. A temperature of 450°C for this transient point was also reported when the concrete was heated to 600ºC [Yu and Lu 2013]. Prokoski [Prokoski 1995] may be the earliest researcher who measured the fracture toughness of ordinary and refractory concretes exposed up to 1300°C at 28 days on the concrete beams under three-point bending. He found the fracture toughness for Mode I, K_{IC}, continuously decreased with the increasing heating temperatures from 0.643 $MNm^{-3/2}$ at 20°C to 0.044 $MNm^{-3/2}$ at 1100°C for the ordinary concrete and from 0.718 $MNm^{-3/2}$ at 20°C to 0.343 $MNm^{-3/2}$ at 1300°C for the refractory concrete. However, an exposure time of 2 hours at high temperatures might not be long enough to obtain a uniform temperature within the concrete specimen and very large thermal and hygric gradients would still exist. In the calculations, only the initial crack length was used but the propagation of the pre-crack was ignored, which led to the values of K_{IC} to be geometrically dependent. Hamoush [Hamoush et al 1998] measured the residual fracture toughness of normal strength crushed limestone concrete on forty-five edge-notched beams under three-point bending by considering a process zone (crack extension zone) at the peak load and found that K_{IC} monotonically decreased with increasing temperatures. The maximum heating temperature in his study was only 300ºC so the application of his test results is limited. Meanwhile, the effect of self-weight of the beam was not considered even though this effect would become more significant with the increasing heating temperature. This would lead to the test data to be less accurate. Zhang [Zhang et al 2002a] investigated the classic fracture toughness, K_{IC}, and the fracture energy related fracture toughness, K_{IC}', for assessing the residual fracture toughness of heated normal- and high-strength concrete. K_{IC} is an instantaneous parameter that represents the crack resistance of concrete at the peak load, while K_{IC}' is a synthetic process parameter that represents the crack resistance over the whole failure process. The effects of heating temperature, exposure time and curing age on the fracture toughness were experimentally investigated and analysed by conducting three-point bending tests on eighty-seven notched normal- and high-strength concrete beams that had been heated between 100ºC and 600ºC over various exposure times up to 168 hours and cooled down to the room temperature. Four testing ages from 7 to 90 days were adopted. Higher heating temperature over 200ºC generally decreased fracture toughness but below 200ºC some strengthening and toughening effect was observed.

Similar phenomenon was found for longer exposure time as well, but such effect was more significant at the early exposure stage under 12 hours. Longer curing age only led to slightly larger toughness in the first 28 days and became little influential thereafter. Weight loss was also measured to distinguish different stages of the fracture toughness of concrete with heating temperatures. The quick evaporation of capillary water hardly affected the fracture toughness but the evaporation of gel water and chemically bound water and the decomposition significantly decreased the fracture toughness.

So far, information about the fracture toughness of concrete exposed to high temperatures is very limited even though K_{IC} can be used to assess the resistance of concrete against cracking and failure at high temperature. The determination of the fracture process zone size will be very important for accurately calculating the fracture toughness at high temperatures. Hence, more work needs to be done to further study the effect of various heating scenarios on the fracture toughness of concrete at high temperatures. The effect of moisture migration on the fracture toughness also needs to be further investigated.

The whole test programme was divided into several series. Each series was specially designated to target one parameter which would largely influence the fracture toughness and other fracture properties of high performance concrete. These included the heating temperature T_m, the testing conditions (hot and cold), the heating rate, the cooling rate (cooling methods) and the exposure time at the designated temperature. In this paper, the test results regarding the effects of the heating temperature T_m and the testing conditions (hot or cold) on the fracture toughness and other properties of the concrete are presented. Those effects were investigated by conducting three-point bending tests on the notched beams of high performance concrete in a furnace. Beside the fracture toughness K_{IC} as a primary parameter, the compressive strength f_{cu}, the splitting tensile strength f_t', the modulus of rupture f_r, the fracture toughness G_F and the Young's modulus E were also studied. K_{IC}, G_F and f_r were measured under both hot and cold conditions, whereas other properties were measured after cooling (residual). The weight loss ω was continuously measured during the time when the concrete was heated and could be used to further study its effect on the fracture behaviour of concrete during heating. Thus, the relationships of K_{IC} and other properties with T_m, the testing conditions (hot and cold) and ω could be established.

2. FRACTURE MECHANICS AND FRACTURE TOUGHNESS

2.1 Application of Fracture Mechanics to Concrete

Since Kaplan first measured the fracture toughness and strain energy release rate of concrete in the early 1960s [Kaplan 1961], much theoretical and experimental work has been done to assess whether linear elastic fracture mechanics (LEFM) could be directly applied to concrete materials. Concrete is neither a perfect elastic brittle material like glass nor a quasi-brittle material and shows some non-linearity before the peak load is reached. Accordingly the stable crack growth, also termed as the fracture process zone, occurs due to micro cracks in the mortar and bond cracks at the cement paste-aggregate interface, or crack arresting, kinking and linking between aggregate particles, or a macro crack. All of this makes the measured fracture toughness become

geometrically dependent. To accurately determine the fracture toughness of concrete, the stable crack growth has to be added to the initial notch depth and the effective crack length is adopted. Thus, the obtained fracture toughness as a true material property will be fully geometrically independent. Hillerborg used the fictitious crack model to determine fracture energy [Hillerborg et al 1976]. Bažant et al used the size effect model and the crack band model to determine *R*-curve parameters, fracture energy, crack band width, strain softening modulus, etc. [Bažant and Oh 1983; Bažant 1984; Bažant et al 1986; Gettu et al 1990]. Karihaloo and Nallathambi extensively investigated the effects of crack size, water/cement ratio and coarse aggregate texture on the fracture toughness of concrete and proposed the effective crack model based on massive test data for calculating the fracture toughness, and their empirical formulae is very convenient to use [Nallathambi et al 1984; Karihaloo and Nallathambi 1989]. Shah proposed the two-parameter fracture model to work out the effective crack length so as to eliminate the effect of geometry [Shah 1990]. A parameter with length dimension was also used to determine the maximum load, notch sensitivity, *R*-curve, etc. RILEM [RILEM 1990a, 1990b] proposed the drafts for determining the fracture toughness K_{IC} and the critical crack tip opening displacement $CTOD_c$ by using either Shah's two-parameter model [Shah 1990] or Bažant's size effect model [Bažant et al 1986]. Guinea, Planas and Elices [Guinea et al 1992; Planas et al 1992; Elices et al 1992] identified possible sources of the experimental error in the RILEM method [RILEM 1985] for measuring the fracture energy and proposed a method to eliminate the major source of the error by including the work-of-fracture due to practical difficulties in capturing the tail part on the load-deflection curve. Their model was later applied and developed further [Rosselló and Elices 2004; Rosselló et al 2005]. Direct tension [Phillips and Zhang 1993] and splitting tension tests [Ince 2010] were tried to obtain stable fracture toughness of concrete. Xu and Reinhardt proposed the double-*K* fracture model to simulate the fracture of concrete including the initial fracture toughness K_{IC}^{ini} and the unstable fracture toughness K_{IC}^{un} [Xu and Reinhardt 1999a, 1999b, 1999c, 2000]. These two fracture toughness parameters were obtained from the initial fracture energy release rate G_{IC}^{ini} and the unstable fracture energy release rate G_{IC}^{un} measured on compact tension, wedge splitting and three-point bending concrete specimens. Zhao, Kwon and Shah investigated the effect of specimen size on the fracture energy and softening curve of concrete using inverse analysis on the test data [Zhao et al 2008; Kwon et al 2008]. Very recently, Murthy and Karihaloo extensively investigated the size effect on the specific fracture energy of normal and high strength concrete using tri-linear and other methods [Karihaloo et al 2013; Murphy et al 2013].

2.2 Fracture Toughness of Concrete

In the linear fracture mechanics (*LEFM*), the fracture toughness for mode I, K_{IC}, also called the critical stress intensity factor, is generally calculated from

$$K_{IC} = \sigma_N \sqrt{a}\, F(\alpha) \tag{1}$$

where

σ_N is the nominal applied stress,

a is the effective crack length, $a = a_0 + \Delta a$,
a_0 is the initial notch depth,
Δa is the crack propagation at peak load and is also widely regarded as the size of the process zone or crack zone,
α is the effective notch-depth ratio and $\alpha = a/H$,
H is the specimen depth,
$F(\alpha)$ is a geometric function.

Different test methods can be used to determine K_{IC} and the three-point bending test on a single-edge notched beam is the most popular one. Fig. 1 shows the arrangement of the three-point bending test on a notched concrete beam. Thus, σ_N in Eq. (1) is equal to the modulus of rupture of the corresponding un-notched beam and can be expressed by considering the self-weight of the beam as

$$\sigma_N = \frac{6M}{BH^2} = \frac{1.5(P_u + P_0)S}{BH^2} = \frac{1.5[P_u + 0.5\,m\,g\,(L/S)(2 - L/S)]S}{BH^2} \qquad (2)$$

where
B is the width of the beam,
L is the full length of the beam,
S is the effective span,
M is the maximum moment at the middle span, given by $M = (P_u + P_0)S/4$,
P_u is the maximum load at peak,
P_0 is the equivalent load due to the self-weight of the beam and $P_0 = 0.5\,m\,g\,(L/S)(2 - L/S)$,
m is the mass of the beam between the supports and is calculated as $m = m_0\,(S/L)$,
m_0 is the total mass of the beam,
g is the acceleration due to gravity and $g = 9.81$ m/s^2.
Here, the factor $(L/S)(2 - L/S)$ is used to eliminate the influence of the cantilever parts of the concrete beam outside the supports.

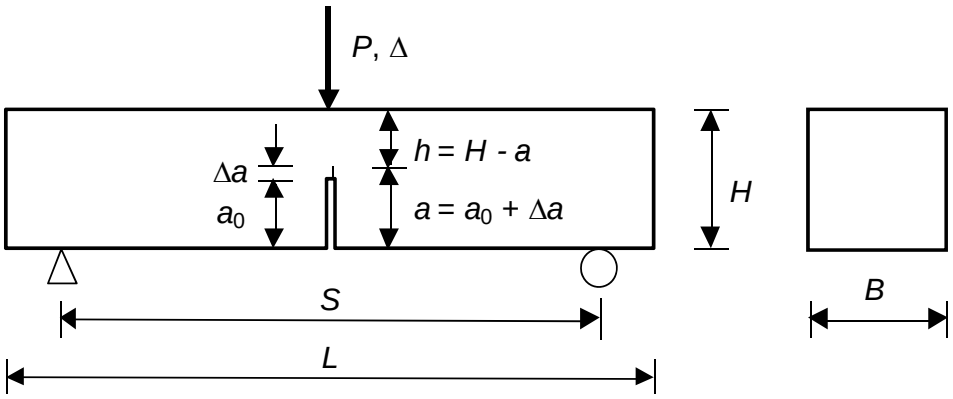

Fig. 1 Dimensions of a single edge notched beam in three-point bending

Here the ligament height h is equal to $H - a$. At high temperatures, the self-weight of the beam will no longer be constant but very much depend on the heating scenario. Hence m should be replaced by the actual mass m' which is defined as

$$m' = m\,(1-\omega) \tag{3}$$

where ω is the percentage weight loss during heating, greatly dependent on heating scenarios. For $S/H = 4$, the geometric function $F(\alpha)$ can be expressed as [Karihaloo and Nallathambi 1989; RILEM 1990a]

$$F(\alpha) = \frac{1.99 - \alpha\,(1-\alpha)\,(2.15 - 3.93\,\alpha + 2.70\,\alpha^2)}{(1+2\,\alpha)\,(1-\alpha)^{3/2}} \tag{4}$$

Different models have been proposed to calculate the effective crack length a, including Bažant's size effect model [Bažant et al 1986], Shah's two parameter model [Shah 1990], Karihaloo's empirical model [Nallathambi et al 1984; Karihaloo and Nallathambi 1989], etc. All these models give very similar results. In Bazant's model, a cannot be directly obtained and a series of tests need to be conducted to determine the parameters. In Shah's model, sometimes a servo test machine has to be used to obtain a stable load-displacement curve and carry out unloading at or soon after the peak load to obtain the instantaneous compliance. However, Karihaloo's model is more simple and direct so it is adopted in this study. From this model, the effective crack length a can be obtained from

$$\frac{a}{H} = \gamma_1 \left(\frac{\sigma_N}{E}\right)^{\gamma_2} \left(\frac{a_0}{H}\right)^{\gamma_3} \left(1+\frac{d}{H}\right)^{\gamma_4} \tag{5}$$

where

d is the maximum aggregate size used in the concrete mix,

E is the Young's modulus of concrete,

γ_1 to γ_4 are constants and can be obtained from the best fit of test data.

When E is obtained from separate tests, $\gamma_1 = 0.198$, $\gamma_2 = -0.131$, $\gamma_3 = 0.394$ and $\gamma_4 = 0.600$ [Karihaloo and Nallathambi 1989]. In this model, the material role is governed by the elastic deformability σ_N/E and the texture heterogeneity through the aggregate size d. The latter is likely to be affected by thermal damage as well. Here, the effect of heating temperature is only considered in the σ_N/E ratio.

In the process for determining K_{IC}, σ_N is first calculate using Eq. (2), then followed by determining $\alpha = a/H$ using Eq. (5) and $F(\alpha)$ using Eq. (4), and finally calculating K_{IC} using Eq. (1). The modulus of rupture f_r for the notched beam can be determined as

$$f_r = \frac{6\,M}{B\,(H-a_0)^2} = \frac{1.5\,(P_u + P_0)\,S}{B\,(H-a_0)^2} = \frac{1.5\,[P_u + 0.5\,m\,g\,(L/S)\,(2-L/S)]\,S}{B\,(H-a_0)^2} \tag{6}$$

In this study, $a_0/H = 0.5$ so $f_r = 4\sigma_N$.

The fracture energy, G_F, defined as the total energy dissipated over a unit area of the cracked ligament, was obtained on the basis of the work done by the force (the area under a load-displacement curve (P – Δ curve) in three-point bending on a centrally notched beam) associated with the gravitational work done by the self-weight of the beam. G_F was calculated based on the following formula:

$$G_F = \frac{\int_0^{\Delta_0} P(\Delta)\, d\Delta + m' g\, (L/S)\,(2 - L/S)\,\Delta_0}{B\,(H - a_0)} \tag{7}$$

Here, Δ_0 is the ultimate displacement when the beam is broken.

The fracture toughness can also be calculated using the fracture energy G_F and the Young's modulus E in LEFM, termed as K_{IC}' to distinguish from the classic fracture toughness K_{IC}, as follows

$$K_{IC}' = \sqrt{G_F\, E} \tag{8}$$

The classic fracture toughness K_{IC} is obtained based on the ultimate load on the ascending branch of a load-displacement curve, including linear loading and hardening. It can be used to reflect the resistance of concrete against cracking. However, it cannot represent the crack resistance of the heated concrete over the whole loading process because it neglects the resistance after the peak load, i.e. softening property. In other words, the crack resistance of concrete can be represented using load capacity and deformation ability, i.e. energy dissipation. This resistance can be well reflected using the fracture energy G_F. If the stiffness change is included, the fracture toughness of concrete exposed to high temperatures can be more reasonably described. Thus, the fracture toughness related to fracture energy, K_{IC}', can play this important role. Because K_{IC}' can represent the behaviour of concrete at both ascending and descending branches of the complete loading process including linear, hardening and softening, its magnitude can be expected to be larger than K_{IC} but its physical meaning can be more reasonable and meaningful.

3. EXPERIMENTAL

3.1 Concrete Specimens

Eight heating temperatures were adopted as T_m = 105ºC, 150ºC, 200ºC, 250ºC, 300ºC, 350ºC, 400ºC and 450ºC, respectively, with a constant heating rate of $\dot{T}^+$ = 3ºC/min for a fixed exposure time of 16 hours. Cooling was achieved by leaving the furnace fully closed to obtain slow cooling conditions. A total of eighty beams were tested with at least three beams for each scenario, and prisms were tested for measuring the residual Young's modulus. As bench marks, five beams and three prisms were tested at 20ºC.

The primary fracture parameters measured under both hot and cold conditions were the fracture toughness K_{IC}, the fracture energy G_F and the modulus of rupture f_r. The residual material properties measured were the compressive strength f_{cu}, the splitting

tensile strength f_t', the Young's modulus E and the concrete density ρ. The weight loss ω was continuously measured during the time when the concrete was heated and could be used to further study its effect on the fracture behaviour of concrete during heating. Part of the test data for the above mentioned parameters for different heating scenarios have been reported in other publications [Zhang and Bićanić 2006; Zhang 2011; Zhang et al 2013].

Notched concrete beams of 500 mm × 100 mm × 100 mm, with a 400 mm effective span and a 50 mm notch depth, were loaded under three-point bending for determining G_F, K_{IC} and f_r. Notches were prepared using a diamond saw before being heated. Concrete prisms of 200 mm × 100 mm × 100 mm were cast for determining the residual E, three for each scenario. To effectively utilise the heated concrete, 100 mm cubes were cut from the broken beams for obtaining f_{cu} and f_t'.

The 42.5N OPC and PFA were adopted as adhesive materials. The aggregates included the calcareous quartz sand, the 10 mm single-sized and 20 mm graded quartz dolerite. Pozzolith 300 N plasticiser was used for achieving a slump of 125 mm. The concrete mix design is listed in Table 1. The test age was at least 90 days to allow full hydration, giving f_r = 6.35 MPa, f_{cu} = 67.1 MPa, f_t' = 4.47 MPa, E = 35.6 GPa, ρ = 2463 kg/m^3, G_F = 228.2 N/m, K_{IC} = 1.389 MN/m$^{1.5}$ and K_{IC}' = 2.845 MN/m$^{1.5}$.

Table 1 Concrete mix design in weight

Contents	OPC	PFA	Quartz sand	10 mm dolerite	20 mm dolerite	Water	Plasticiser
Weight ratio	1	0.33	2.45	1.39	2.78	0.56	0.006
Quantities (kg/m^3)	300	99	735	417	834	168	1.8

3.2 Heating Furnace and Testing Facility

A program-controlled three-zone VTS furnace (600 ± 5ºC) was specially designed and it had two identical halves with an overall inner dimension of 800 mm × 600 mm × 600 mm. Fans were used to circulate the air in the furnace for heating the concrete uniformly and cooling the loading pieces. The furnace was built around a 2000 kN LOS universal testing machine to allow the tests to be conducted at high temperatures. Fig. 2 shows the furnace with the testing machine and the control panel.

A high-yield steel loading piece, including bottom block and top plate, was designed to allow two beams to be tested while being hot in one heating batch. The bottom block was connected to the lower actuator of the machine. The top plate could slide against the block after it was slightly raised by using two lifting bars. Prior to heating, two beams were put on the loading piece symmetrically in the furnace. When the heating process was completed, one beam was lifted to the centre of the machine and then tested. The second beam could then be lifted to the centre for testing. High yield steel was also used for the top piece which was connected to the upper actuator. According to the requirement by RILEM [RILEM 1985], the roller bearing was used for one support for each beam and the ball bearing for the other support. Fig. 3 illustrates the top and bottom loading pieces with the twin concrete specimens.

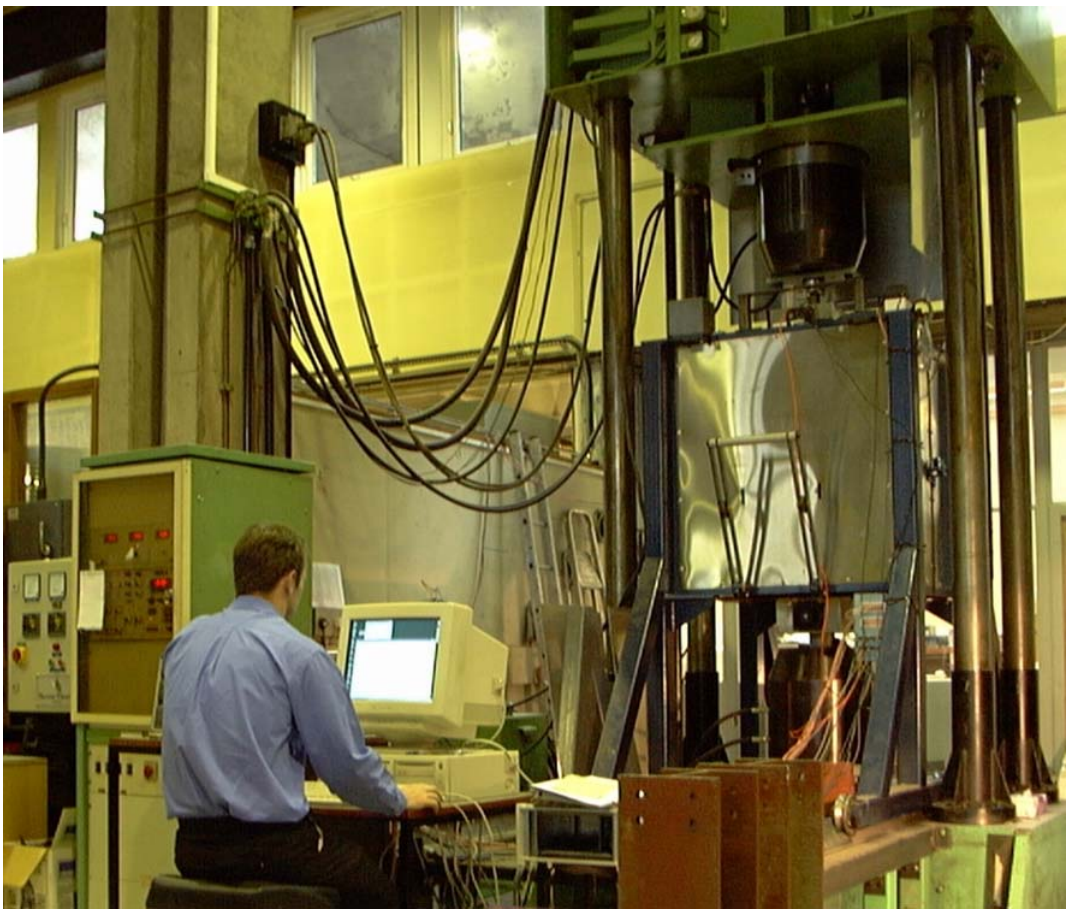

Fig. 2 A programme-controlled furnace with the 2000 kN LOS testing machine

A 10 kN high temperature load cell, located outside the furnace, was inserted between the top piece and top actuator for load measurement due to its working limit of 180ºC and continuously cooled during the heating-testing process so that the actual temperature in the load cell was below 50°C. The displacement of the machine was automatically recorded using a built-in displacement transducer. Four LIN high temperature linear voltage displacement transducers (LVDTs) with a working temperature of 600°C were also used for monitoring the creep of the concrete during heating, two for each beam.

Three-point bending tests at high temperatures and after cooling were conducted at a displacement rate of 1.25×10^{-3} mm/s. The load and displacements were recorded using a data logger at a rate of two sets per second. Each test took 10 to 15 minutes.

To monitor the temperature developments in the concrete, N-type thermocouples were embedded in the beams for three-point bending tests. Two positions were chosen for each beam: 50 mm close to the edge (side hole) and 50 mm away from the centre (middle hole) to avoid disturbing the notched mid-section. The 50 mm deep holes were drilled before the beams were heated. The temperatures from the thermocouples in the three heating zones and from the master thermocouple of the furnace were recorded.

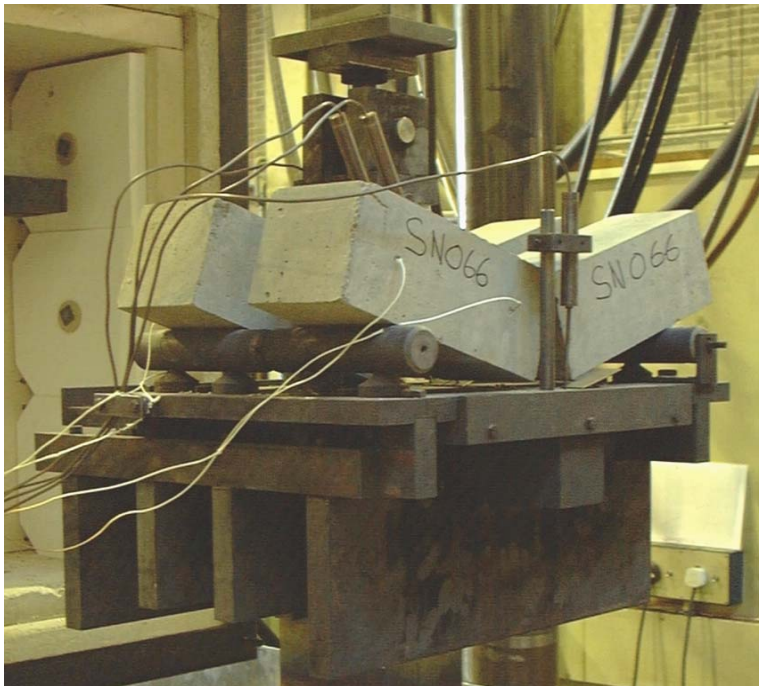

Fig. 3 N-type thermocouples embedded in the beam specimens

3.3 Weight Loss Measurement

For continuously monitoring of moisture migration during heating, exposure, testing and cooling, two steel cradles were made for hanging concrete beams, each connected to a VC8000 high precision load cell of 25 kg $\pm$ 10 g, fixed outside the furnace. During heating, exposure and cooling, the weight changes were recorded at the same rates as those for temperatures.

4. FRACTURE TOUGHNESS K_{IC} AND K_{IC}'

4.1 Summary of the Previous Study

The effects of the heating temperature on the fracture energy and other mechanical properties of the high performance concrete at high temperatures up to 450ºC under hot and cold conditions were reported in the previous publications [Zhang and Bićanić 2006; Zhang 2011]. The main findings are summarised as follows.

The measurements using thermocouples indicated that the temperature in the concrete always developed behind the furnace temperature but a thermal equilibrium could be reached if the exposure time was long enough.

The weight loss monotonically increased with the increasing heating temperature. High heating temperatures always led to large weight losses but a hygric equilibrium state could be reached if the exposure time was long enough, in particular for low heating temperatures, e.g. 16 hours for obtaining a hygric equilibrium state in this study.

The fracture energy generally sustained a decrease-increase tendency with the heating temperature for the hot concrete but a hold-increase-decrease tendency for the cold concrete. The fracture energy changed with the ultimate weight loss in a similar way. At the first stage, the evaporation of capillary water at low heating temperatures only slightly affected the fracture energy but the later evaporation of the gel water and chemically combined water and decomposition significantly reduced the fracture energy.

The modulus of rupture decreased with the increasing heating temperature for the hot concrete, but sustained an increase-decrease tendency for the cold concrete. There was a sudden drop at 105ºC for the hot concrete due to high vapour pressure inside the concrete. There existed a tri-linear decrease-recovery-decrease trend between the modulus of rupture and the ultimate weight loss for the hot concrete and a bi-linear increase-decrease trend for the cold concrete.

Both residual compressive and tensile strengths decreased with the increasing heating temperature. There was a sudden drop in the concrete strengths between 105ºC and 150ºC due to the residual stress caused by the high vapour pressure inside the concrete. Tensile strength decreased more rapidly than compressive strength for the same heating scenario. Concrete strengths had two-stage decrease tendencies related to the ultimate weight loss.

The residual Young's modulus of concrete monotonically decreased with the increasing heating temperature and this could be expressed by using a linear relationship. There existed a two-stage linear relationship between the residual Young's modulus and the ultimate weight loss.

4.2 K_{IC} and K_{IC}' versus T_m

Fig. 4 shows K_{IC} and K_{IC}' for various heating temperatures and testing conditions. In general, both K_{IC} and K_{IC}' decreased with the increasing hearing temperature but followed different tendencies.

For the hot concrete, K_{IC} sustained a decrease-recovery-decrease tendency but generally followed a decreasing tendency with increasing T_m. K_{IC} decreased from 1.389 MN/m$^{1.5}$ at 20ºC to 1.101 MN/m$^{1.5}$ at 105ºC with a sudden drop of 21%, due to high vapour pressures inside the concrete, but recovered to 1.243 MN/m$^{1.5}$ at 150ºC. It then continuously decreased to 1.223 MN/m$^{1.5}$ at 200ºC, 1.081 MN/m$^{1.5}$ at 300ºC and 0.866 MN/m$^{1.5}$ at 450ºC with a net drop of 38%.

For the cold concrete, K_{IC} first decreased slowly with T_m. At 150ºC, K_{IC} only slightly decreased from 1.389 MN/m$^{1.5}$ at 20ºC to 1.316 MN/m$^{1.5}$, down by 0.073 MN/m$^{1.5}$ or 5%. Thereafter it more rapidly decreased with T_m, down to 1.227 MN/m$^{1.5}$ at 200ºC and 0.996 MN/m$^{1.5}$ at 300ºC. At 450ºC, K_{IC} decreased to 0.771 MN/m$^{1.5}$, with a net drop of 0.618 MN/m$^{1.5}$ or 45% which was larger than that for the hot concrete. This means that cooling would cause further damage to the concrete by forming more micro-cracks.

Fig. 4 also shows that for $T_m \leq 200$ºC, the values of K_{IC} for the hot concrete were smaller than those for the cold concrete. At this stage, the high vapour pressure under hot conditions could not efficiently evaporate so as to significantly reduce the fracture toughness of the concrete. The cooling process eliminated the vapour pressure and did not damage the concrete. For higher heating temperatures over 200ºC, the values of K_{IC} for the hot concrete were larger than those for the cold concrete. At this stage, there

were no longer high vapour pressures within the concrete because micro cracks had already formed. However, cooling would cause more micro cracks and further damage the concrete. Thus, even smaller fracture toughness would be expected.

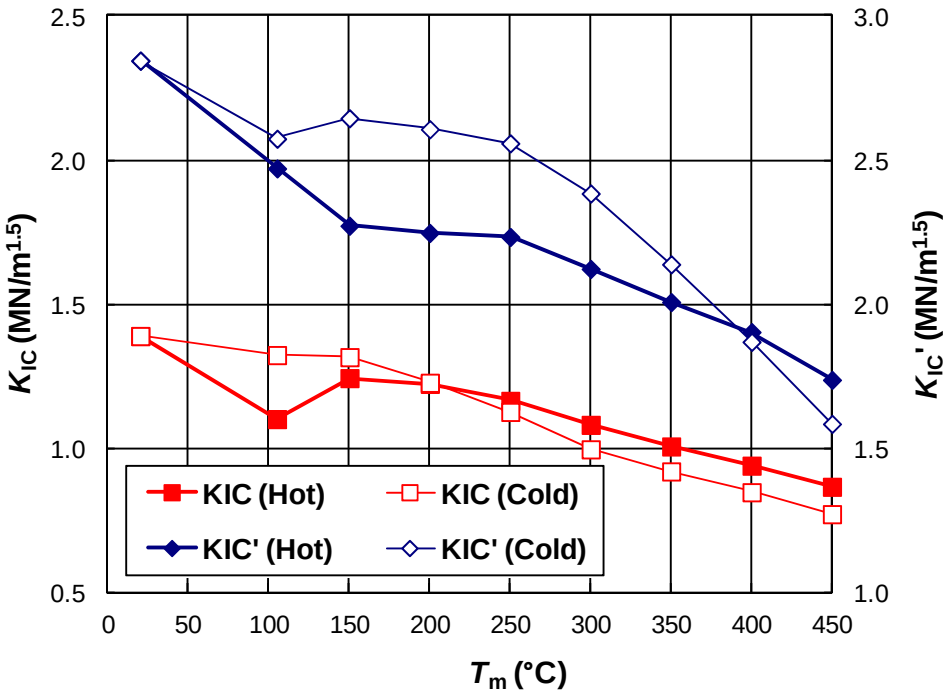

Fig. 4 K_{IC} and K_{IC}' for different heating temperatures and testing conditions

From Fig. 4, it can be seen that the values of K_{IC}' were twice as large as the values of K_{IC} for all heating temperatures and different testing conditions. As mentioned above, K_{IC} is an instantaneous parameter and represents the cracking resistance at the peak load, while K_{IC}' is a more synthetic process parameter and represents the resistance over the whole fracture process.

For the hot concrete, K_{IC}' sustained a decrease-hold-decrease tendency but generally followed a decreasing tendency with increasing T_m. K_{IC}' decreased from 2.845 MN/m$^{1.5}$ at 20ºC to 2.272 MN/m$^{1.5}$ at 105ºC, but was almost unchanged until 250ºC with a value of 2.233 MN/m$^{1.5}$. Thereafter it continuously decreased to 2.122 MN/m$^{1.5}$ at 300ºC and 1.737 MN/m$^{1.5}$ at 450ºC with a net drop of 39%.

For the cold concrete, K_{IC}' has a sudden drop at 105ºC from 2.845 MN/m$^{1.5}$ at 20ºC to 2.574 MN/m$^{1.5}$, down by 0.271 MN/m$^{1.5}$ or 10%. It recovered to 2.645 MN/m$^{1.5}$ at 150ºC and then slowly decreased until 250ºC with a value of 2.558 MN/m$^{1.5}$. Thereafter, K_{IC}' continuously decreased at a high rate to 2.138 MN/m$^{1.5}$ at 350ºC and 1.584 MN/m$^{1.5}$ at 450ºC, with a net drop of 1.261 MN/m$^{1.5}$ or 44%. For most heating temperatures, the values of K_{IC}' for the hot concrete were always smaller than those for the cold concrete except for $T_m \geq$ 400ºC.

4.3 K_{IC} and K_{IC}' versus ω_u

Fig. 5 shows the relationships of K_{IC} and K_{IC}' with the ultimate weight loss ω_u for hot and cold testing conditions. In general, both K_{IC} and K_{IC}' decreased with the increasing hearing temperature but followed different tendencies.

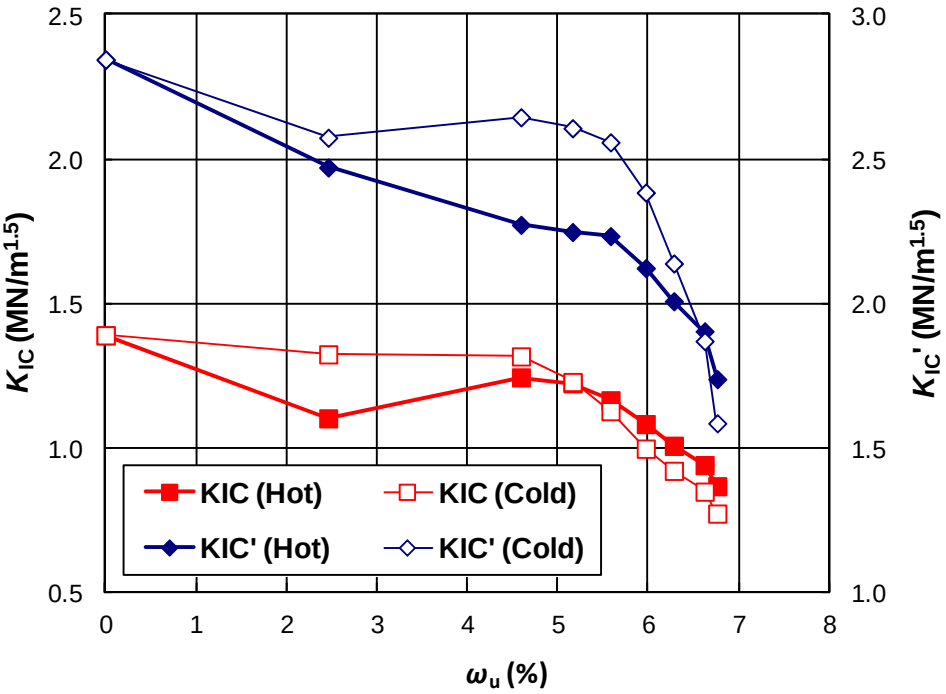

Fig. 5 K_{IC} and K_{IC}' versus ultimate weight loss ω_u

For the hot concrete, K_{IC} had a decrease-recovery-decrease tendency with ω_u. K_{IC} sharply decreased with ω_u first from 1.389 MN/m$^{1.5}$ at 20ºC to 1.101 MN/m$^{1.5}$ at 105ºC with a toughness loss of 21%, corresponding to a threshold weight loss ω_{u1} = 2.46%. At the second stage, K_{IC} quickly recovered to 1.243 MN/m$^{1.5}$ at 150ºC with ω_{u2} = 4.59%. Thereafter, K_{IC} continuously decreased with ω_u again. This tendency can be expressed using a tri-linear relationship. For the cold concrete, K_{IC} sustained a two-stage slow decrease - fast decrease tendency with ω_u. It slightly decreased with ω_u until 150ºC with ω_{u2} = 4.59% and then continuously decreased with ω_u. A bi-linear K_{IC} – ω_u relationship can be used for the cold concrete. Similarly, for $\omega_u \le \omega_{u3}$ = 5.16% corresponding to $T_m \le$ 200ºC, the values of K_{IC} for the hot concrete were smaller than those for the cold concrete. For higher weight loss over ω_{u3} = 5.16% or higher heating temperatures over 200ºC, the values of K_{IC} for the hot concrete were larger than those for the cold concrete.

Also for the hot concrete, K_{IC}' had a slow decrease - fast decrease tendency with ω_u. K_{IC}' continuously but slowly decreased with ω_u first from 2.845 MN/m$^{1.5}$ at 20ºC to 2.233 MN/m$^{1.5}$ at 250ºC with a toughness loss of 22%, corresponding to a threshold weight loss ω_{u4} = 5.58%. At the second stage, K_{IC}' continuously but quickly decreased with ω_u. This tendency can be expressed using a bi-linear relationship. For the cold

concrete, K_{IC}' sustained a three-stage decrease-hold-decrease tendency with ω_u. It slightly decreased with ω_u until 105ºC with ω_{u1} = 2.46% and then was almost unchanged until ω_{u4} = 5.58% corresponding to 250ºC. Thereafter K_{IC}' rapidly decreased with ω_u. A tri-linear K_{IC}' – ω_u relationship can be used for expressing the trend for the cold concrete. Similarly, for $\omega < \omega_{u5}$ = 6.62% corresponding to T_m < 400ºC, the values of K_{IC}' for the hot concrete were smaller than those for the cold concrete. For higher weight loss over ω_{u5} = 6.62% or higher heating temperatures, the values of K_{IC}' for the hot concrete were larger than those for the cold concrete.

4.4 K_{IC} versus f_r

Fig. 6 illustrates a relationship between K_{IC} and f_r for all the heating temperatures and testing conditions. It can be seen that all the test results can be represented by a linear equation as

$$K_{IC} = 0.192\, f_r \quad \text{or} \quad K_{IC} = 0.768\, \sigma_N \tag{9}$$

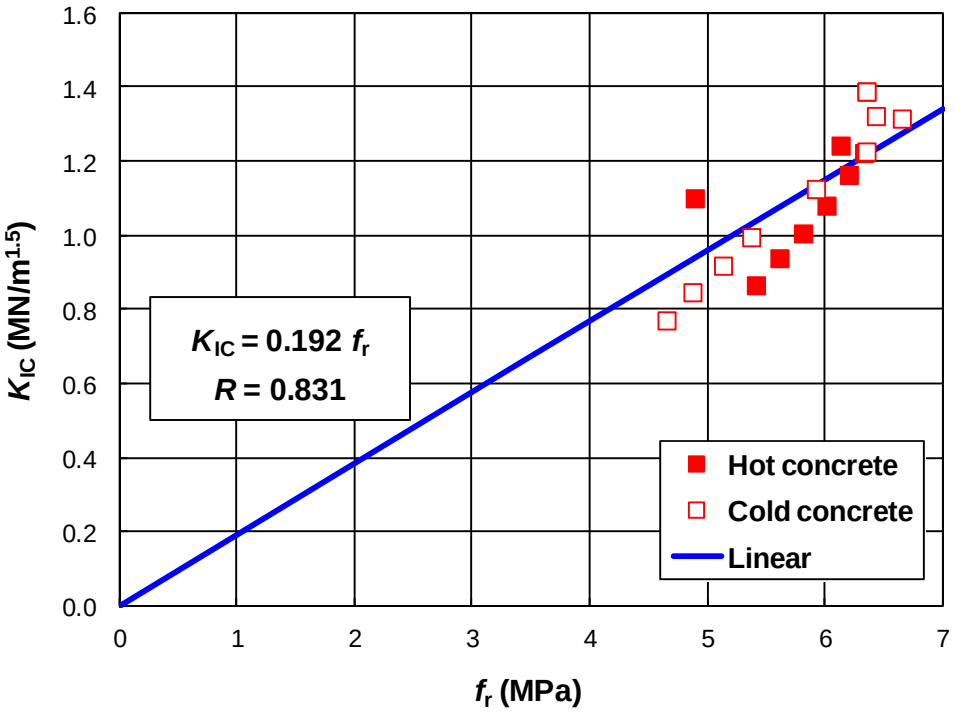

Fig. 6 Relationship between K_{IC} and f_r for different heating temperatures

with a linear correlation coefficient R = 0.831. This relationship can also be directly confirmed from Eq. (1). In comparison with Eq. (1), the term $\sqrt{a}\,F(\alpha)$ can be obtained as 0.768. This means that for a given material and geometry, the classic fracture toughness K_{IC} can estimated by the modulus of rupture of the notched beam. In this study, however, the correlation between the fracture toughness K_{IC} and the modulus of rupture f_r was not as good as that reported in the previous study on the residual fracture

properties of the normal- and high-strength concrete subjected to high temperatures by the authors [Zhang and Bićanić 2002a]. This is because the majority of f_r values fell within 4.0 to 7.0 MPa rather than largely distributed even though K_{IC} varied reasonably largely with the heating scenarios.

5. CONCLUSIONS

In this study, the fracture toughness K_{IC} of high performance concrete was evaluated by conducting three-point bending tests on eighty notched beams at high temperatures up to 450ºC (hot) and in cooled-down states (cold). The exposure time was maintained as 16 hours, and both thermal and hygric equilibriums were achieved.

K_{IC} for the hot concrete sustained a monotonic decrease tendency with the heating temperature, except for a sudden drop at 105ºC. For the cold concrete, K_{IC} sustained a two-stage decrease trend, dropping slowly with the heating temperature up to 150ºC and rapidly thereafter. When $T_m \leq 200$ºC, K_{IC} for the hot concrete was smaller than that for the cold concrete, and a reverse trend occurred for higher heating temperatures.

For both hot and cold concrete, K_{IC}' sustained a decrease-hold-decrease tendency with T_m. For most heating temperatures, K_{IC}' for the hot concrete was always smaller than that for the cold concrete except for $T_m \geq 400$ºC.

K_{IC}' was twice as large as K_{IC} for all heating temperatures because K_{IC} is an instantaneous parameter and represents the cracking resistance at the peak load, while K_{IC}' is a more synthetic process parameter and represents the resistance over the whole fracture process.

For the hot concrete, K_{IC} sustained a decrease-recovery-decrease tendency with ω_u. In the first two stages, K_{IC} only slightly decreased until 150ºC and then dropped rapidly with ω_u. K_{IC} for the cold concrete clearly followed a two stage decrease trends, dropping slowly first and then rapidly after 150ºC.

For the hot concrete, K_{IC}' sustained a two stage decrease tendency with ω_u. K_{IC}' first slowly decreased with ω_u until 250ºC. At the second stage, K_{IC}' continuously but quickly decreased with ω_u. For the cold concrete, K_{IC}' sustained a three-stage decrease-hold-decrease tendency with ω_u. It slightly decreased with ω_u until 105ºC and then was almost unchanged until 250ºC. Thereafter K_{IC}' rapidly decreased with ω_u.

A fairly linear relationship between K_{IC} and f_r existed for the test results in this study.

ACKNOWLEDGEMENTS

This project was conducted under the British Energy contract PP/120543/DGD/HN.

REFERENCES

Abe, T., Furumura, F., Tomatsuri, K., Kuroha, K. and Kokubo, I. (1999) “Mechanical properties of high strength concrete at high temperatures,” *J. of Structural and Construction Engineering*, Architectural Institute of Japan, **515**, 163-168.

Baker, G. (1996) “The effect of exposure to elevated temperatures on the fracture energy of plain concrete,” *RILEM Materials and Structures*, **29**, 383-388.

Bangi, M.R. and Horiguchi, T. (2011) “Pore pressure development in hybrid fibre-reinforced high strength concrete at elevated temperatures,” *Cement and Concrete Research*, **41**, 1150-1156.

Bažant, Z.P. and Oh, B.H. (1983) “Crack band theory for fracture of concrete,” *RILEM Materials and Structures*, **16**(93), 155-77.

Bažant, Z.P. (1984) “Size effect in blunt fracture: concrete rock and metal,” *ASCE J. of Engineering Mechanics*, **110**(4), 518-35.

Bažant, Z.P., Kim, J.-K. and Pfeiffer, P.A. (1986) “Nonlinear fracture properties from size effect tests,” *ASCE J. of Structural Engineering*, **112**(2), 289-307.

Bažant, Z.P. and Prat, P.C. (1988) “Effect of temperature and humidity on fracture energy of concrete,” *ACI Materials J.*, **85**(4), 262-271.

Bažant, Z.P. and Kaplan, M.F. (1996) *Concrete at High Temperatures: Material Properties and Mathematical Models*, Longman Group Limited, Harlow Essex, England.

Chen, B. and Liu, J. (2004) “Residual strength of hybrid-fiber-reinforced high-strength concrete after exposure to high temperatures,” *Cement and Concrete Research*, **34**, 1065-1069.

Cülfik, M.S. and Özturan, T. (2002) “Effect of elevated temperatures on the residual mechanical properties of high-performance mortar,” *Cement and Concrete Research*, **32**, 809-816.

Elices, M., Guinea, G.V. and Planas, J. (1992) “Measurement of the fracture energy using three-point bend tests: Part 3 — Influence of cutting the P-δ tail,” *RILEM Materials and Structures*, **25**, 137–163.

Felicetti, R. and Gambarova, P.G. (1998) “Effects of high temperatures on the residual compressive strength of high-strength siliceous concretes,” *ACI Material J.*, **95**(4), 395-406.

Gettu, R., Bažant, Z.P. and Karr, M.E. (1990) “Fracture properties and brittleness of high-strength concrete,” *ACI Materials J.*, **87**(6), 608-618.

Guinea, G.V., Planas, J. and Elices, M. (1992) “Measurement of the fracture energy using three-point bend tests: Part 1 — Influence of experimental procedures,” *RILEM Materials and Structures*, **25**, 212–218.

Haghighi, A., Koohkan, M.R. and Shekarchizadeh, M. (2007) “Optimising concrete using group method of data handling and genetic programme,” *32nd Conf. on Our World in Concrete and Structures*, Singapore.

Hamoush, S.A., Abdel-Fattah, H. and McGinley, M.W. (1998) “Residual fracture toughness of concrete exposed to elevated temperature,” *ACI Materials J.*, **95**(6), 689-694.

Hillerborg, A., Modeer, M. and Petersson, P.E. (1976) “Analysis of crack formation and crack growth in concrete by means of fracture mechanics and finite elements,” *Cement and Concrete Research*, **6**(6), 773-782.

Ince, R. (2010) “Determination of concrete fracture parameters based on two-parameter and size effect models using split-tension cubes,” *Engineering Fracture Mechanics*, **77**, 2233–2250.

Kanellopoulos, A., Farhat, F.A., Nicolaides, D. and Karihaloo, B.L. (2009) “Effect of elevated temperatures on the residual mechanical properties of high-performance mortar,” *Cement and Concrete Research*, **39**, 1087-1094.

Kaplan, M.F. (1961) “Crack propagation and the fracture of concrete,” *ACI J.*, **58**(5), 591-610.

Karihaloo, B.L. and Nallathambi, P. (1989) “An improved effective crack model for the determination of fracture toughness of concrete,” *Cement and Concrete Research*, **19**, 603-610.

Karihaloo, B.L., Murthy. A.R. and Iyer, N.R. (2013) “Determination of size-independent specific fracture energy of concrete mixes by the tri-linear model,” *Cement and Concrete Research*, **49**, 82-88.

Kwon, S.H., Zhao, Z. and Shah, S.P. (2008) “Effect of specimen size on fracture energy and softening curve of concrete: Part II. Inverse analysis and softening curve,” *Cement and Concrete Research*, **38**, 1061-1069.

Murthy, A.R., Karihaloo, B.L., Iyer, N.R., and Raghu Prasad, B.K. (2013) “Determination of size-independent specific fracture energy of concrete mixes by the two methods,” *Cement and Concrete Research*, **50**, 19-25.

Nallathambi, P., Karihaloo, B.L. and Heaton, B.S. (1984) “Effect of specimen and crack sizes, water/cement ratio and coarse aggregate texture upon fracture toughness of concrete,” *M. of Concrete Research*, **36**(129), 227-236.

Nielsen, C.V. (1995) *Ultra High-Strength Steel Fibre Reinforced Concrete, Part I Basic Strength Properties of Compresit Matrix*, PhD Thesis, Department of Structural Engineering, Technical University of Denmark, Denmark.

Nielsen, C.V. and Bićanić, N. (2003) “Residual fracture energy of high-performance and normal concrete subject to high temperatures”, *RILEM Materials and Structures*, **36**(8), 515-521.

Peng, G.-F., Yang, W.-W., Zhao, J., Liu, Y.-F., Bian, S.-H. and Zhao, L.-H. (2006) “Explosive spalling and residual mechanical properties of fiber-toughened high-performance concrete subjected to high temperatures,” *Cement and Concrete Research*, **36**, 723-727.

Phan, L.T. and Carino, N.J. (1998) “Review of mechanical properties of HSC at elevated temperature,” *ASCE J. of Materials in Civil Engineering*, **10**(1), 58-64.

Phillips, D.V. and Zhang, B. (1993) “Direct tension tests on notched and un-notched plain concrete specimens,” *M. of Concrete Research*, **45**, 25-35.

Planas, J., Elices, M. and Guinea, G.V. (1992) “Measurement of the fracture energy using three-point bend tests: Part 2 — Influence of bulk energy dissipation,” *RILEM Materials and Structures*, **25**, 305–312.

Prokoski, G. (1995) “Fracture toughness of concrete at high temperature,” *J. of Materials Science*, **30**, 1609-1612.

Pu, X. (2012) *Super-High-Strength High Performance Concrete*, CRC Press.

RILEM Technical Committee 50 FMC (1985) “Draft recommendation: determination of the fracture energy of mortar and concrete by means of three-point bend test on notched beams,” *RILEM Materials and Structures*, **18**(106), 285-290.

RILEM Technical Committee 89 FME (1990a) “Draft recommendation: determination of fracture parameters (K^s_{IC} and $CTOD_c$) of plain concrete using three-point bend tests,” *RILEM Materials and Structures*, **23**, 457-460.

RILEM Technical Committee 89 FME (1990b) “Draft recommendation: size-effect method for determining fracture energy and process zone size of concrete,” *RILEM Materials and Structures*, **23**, 461-465.

Rosselló, C. and Elices, M. (2004) “Fracture of model concrete 1. Types of fracture and crack path,” *Cement and Concrete Research*, **34**, 1441-1450.

Rosselló, C., Elices, M. and Guinea, G.V. (2006) “Fracture of model concrete: 2. Fracture energy and characteristic length,” *Cement and Concrete Research*, **36**, 1345-1353.

Schneider, U. (1988) “Concrete at high temperatures - a general review,” *Fire Safety J.*, **13**, 55-68.

Shah, S.P. (1990) “Experimental methods for determining fracture process zone and fracture parameters,” *Engineering Fracture Mechanics*, **35**(1/2/3), 3-14.

Ulm, F.-J. and James, S. (2011) “The scratch test for strength and fracture toughness determination of oil well cements cured at high temperature and pressure,” *Cement and Concrete Research*, **41**, 942-946.

Watanabe, K., Bangi, M.R. and Horiguchi, T. (2013) “The effect of testing conditions (hot and residual) on fracture toughness of fiber reinforced high-strength concrete subjected to high temperatures,” *Cement and Concrete Research*, **51**, 6-13.

Xu, S. and Reinhardt, H.W. (1999a) “Determination of double-K criterion for crack propagation in quasi-brittle materials. Part I: Experimental investigation of crack propagation,” *Inter. J. of Fracture*, **98**, 111-49.

Xu, S. and Reinhardt, H.W. (1999b) “Determination of double-K criterion for crack propagation in quasi-brittle materials. Part II: Analytical evaluating and practical measuring methods for three-point bending notched beams,” *Inter. J. of Fracture*, **98**, 151-77.

Xu, S. and Reinhardt, H.W. (1999) “Determination of double-K criterion for crack propagation in quasi-brittle materials. Part III: Compact tension specimens and wedge splitting specimens,” *Inter. J. of Fracture*, **98**, 179-93.

Xu, S. and Reinhardt, H.W. (2000) “A simplified method for determining double-K fracture parameters for three-point bending tests,” *Inter. J. of Fracture*, **104**, 181-209.

Yan, Y.N., Luo, X. and Sun, W. (2000) “Compressive strength and pore structure of high-performance concrete after exposure to high temperature up to 800ºC,” *Cement and Concrete Research*, **30**, 247-251.

Yu, K. and Lu, Z. (2013) “Determination of residual fracture parameters in post-fire concrete using an energy method,” submitted to *Engineering Fracture Mechanics*.

Zhang, B., Bićanić, N., Pearce, C.J. and Balabanic, G. (2000a) “Residual fracture properties of normal- and high-strength concrete subject to elevated temperatures,” *M. of Concrete Research*, **52**(2), 123-136.

Zhang, B., Bićanić, N., Pearce, C.J., and Balabanic, G. (2000b) “Assessment of toughness of concrete subjected to elevated temperatures from complete load-displacement curve — Part I: General introduction,” *ACI Materials J.*, **97**(5), 550-555.

Zhang, B., Bićanić, N., Pearce, C.J., and Balabanic, G. (2000c) “Assessment of toughness of concrete subjected to elevated temperatures from complete load-displacement curve — Part II: Experimental investigations,” *ACI Materials J.*, **97**(5), 556-566.

Zhang, B. and Bićanić, N. (2002a) “Residual fracture toughness of normal- and high-strength gravel concrete after heating to 600°C,” *ACI Materials J.*, **99**(3), 217-226.

Zhang, B., Bićanić, N., Pearce, C.J. and Phillips, D.V. (2002b) “Relationship between brittleness and moisture loss of concrete exposed to high temperatures,” *Cement and Concrete Research*, **32**, 363-371.

Zhang, B. and Bićanić, N. (2006) “Fracture energy of high-performance concrete at high temperatures up to 450°C: the effects of heating temperatures and testing conditions (hot and cold),” *M. of Concrete Research*, **58**(5), 277-288.

Zhang, B. (2011) “Effects of moisture evaporation (weight loss) on fracture properties of high performance concrete subjected to high temperatures,” *Fire Safety J.*, **46**, 543-549.

Zhang, B., Cullen, M. and Kilpatrick, T. (2013) “Effects of thermal and hygric gradients on the spalling of high performance concrete subjected to elevated temperatures,” *The 2013 Inter. Conf. on Computational Technologies in Concrete Structures*, 8-12 September 2013, Jeju, Korea.

Zhao, Z., Kwon, S.H. and Shah, S.P. (2008) “Effect of specimen size on fracture energy and softening curve of concrete: Part I. Experiments and fracture energy,” *Cement and Concrete Research*, **38**, 1049-1060.